AIAA 2003-1978

Deployable Tensegrity Masts

A.G. Tibert
Royal Institute of Technology
Stockholm, Sweden

and

S. Pellegrino
University of Cambridge
Cambridge, U.K.

44th AIAA/ASME/ASCE/AHS/ASC Structures, Structural Dynamics, and Materials Conference and Exhibit

7−10 April 2003
Norfolk, VA

DEPLOYABLE TENSEGRITY MASTS

A.G. Tibert*

Department of Mechanics, Royal Institute of Technology
SE-100 44 Stockholm, Sweden

S. Pellegrino†

Department of Engineering, University of Cambridge
Trumpington Street, Cambridge, CB2 1PZ, U.K.

Abstract

The tensegrity concept has long been considered as a basis for lightweight and compact packaging deployable structures, but very few studies are available. This paper presents a complete design study of a deployable tensegrity mast with all the steps involved: initial form-finding, structural analysis, manufacturing and deployment. Closed-form solutions are used for the form-finding. A manufacturing procedure in which the cables forming the outer envelope of the mast are constructed by two-dimensional weaving is used. The deployment of the mast is achieved through the use of self-locking hinges. A stiffness comparison between the tensegrity mast and an articulated truss mast shows that the tensegrity mast is weak in bending.

Introduction

Tensegrity structures consist of tension elements (cables) forming a continuous network supported and prestressed by discontinuous compression elements (struts). The word *tensegrity* is a contraction of *tens*ile int*egrity*. A definition by Miura and Pellegrino[1] classifies a tensegrity structure "as any structure realised from cables and struts, to which *a state of prestress is imposed that imparts tension to all cables*" with the addition that "as well as imparting tension to all cables, the state of prestress serves the purpose of *stabilising the structure*, thus providing first-order stiffness to its infinitesimal mechanisms." The origin of tensegrity can be pin-pointed to 1921 and the work of the Russian sculptor Ioganson, but today it is generally regarded that Snelson's structure *X-Piece* represents the birth of the concept. Fuller[2] was the first to look upon tensegrity structure from an engineering point of view, but even though the concept is more than fifty years old only a few engineering applications exist.

In recent years the concept has received new attention from scientists in various fields. In the field of deployable aerospace structures a significant number of publications,[3,4] reports[5–7] and patents[8–10] on tensegrity have recently appeared.

Concerning deployability, a key attraction of the tensegrity concept is the disjointed struts, which enable a compact package. The first obstacle in the design of tensegrity structures is finding a prestressed equilibrium configuration. Several methods are available,[11,12] but a single method suitable for general problems does not yet exist. This is an additional step in comparison with traditional deployable masts and adds complexity to the already complicated design of deployable structures. However, the crucial design step is the creation of mechanisms that enable reliable folding/deployment; in the few studies concerned with deployable tensegrity structures[7,13,14] various approaches have been tested. Here, an approach, involving a self-locking hinge, is proposed.

Topology and Form-Finding

In any mast design, finding a suitable element topology is the first task. Compared to other masts, the number of topology schemes for tensegrity masts is restricted since they must be prestressed; at each node the prestressing forces must equal to zero. Various schemes for constructing tensegrity structures are presented by Pugh.[15] Snelson[16] describes the construction of complex tensegrity structures from simple modules. One of the structures is a mast with three struts per stage, Figure 1. However, the number of struts per stage is not restricted to three, any number v is possible. The Snelson masts are created by assembling tensegrity prisms with v struts per stage on top of each other. The prisms are rotated alternately clockwise and counter-clockwise.

*Research Associate, Member AIAA. gunnar.tibert@mech.kth.se
†Professor of Structural Engineering, Associate Fellow AIAA.

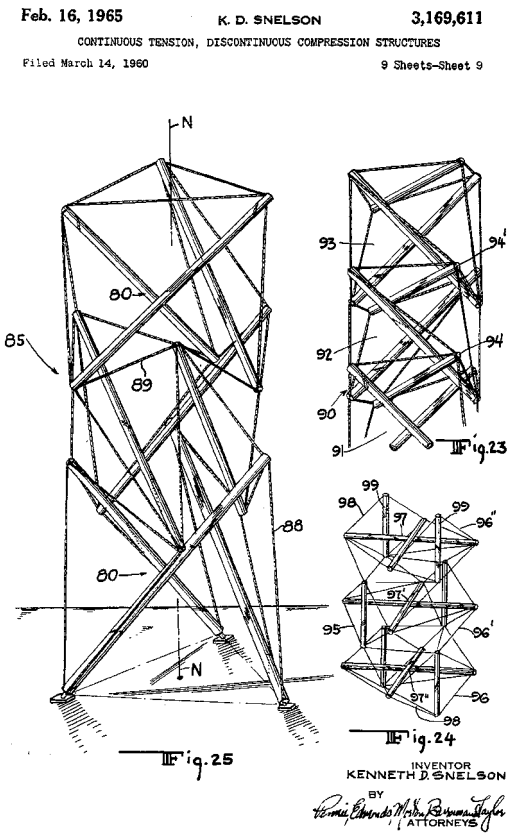

Figure 1: Kenneth Snelson's three-stage tensegrity mast.[16]

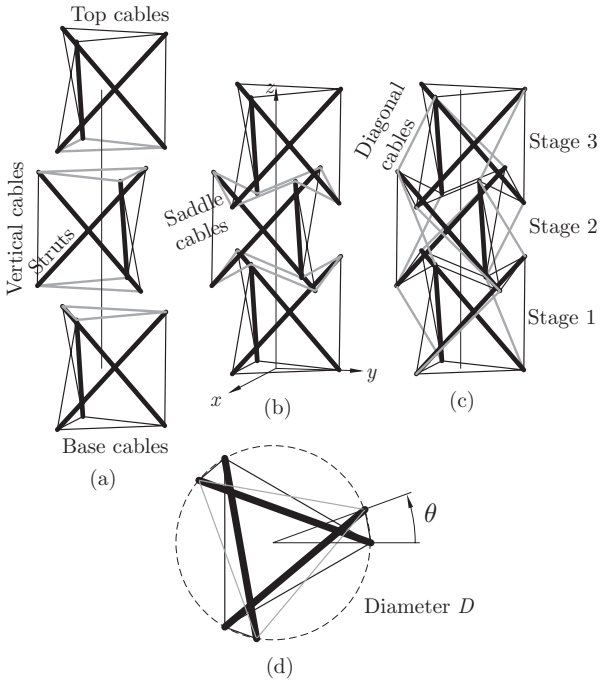

Figure 2: Assembling a three-stage tensegrity tower with three struts per stage from basic tensegrity modules: (a) three modules are (b) assembled by replacing the cables of the bases with saddle cables and finally (c) adding diagonal cables to prestress the structure. The top bases of the top and bottom modules are rotated through an angle θ w.r.t. the bottom base. The middle module is rotated counterclockwise through the same angle.

This procedure is illustrated in Figure 2 for a three-stage mast with three struts per stage. The prisms merge into a mast by substituting their individual base cables with saddle cables and adding diagonal cables for further stiffening. The height of each module is H, but the height of the three-stage mast is lower than $3H$ due to the overlap h of the saddle cables.

Tensegrity masts with other configurations are available: Furuya[13] assembles tensegrity prisms directly on top of each other and Fuller[2] presents a tetrahedral tensegrity mast. Both of these masts have connected struts and are, in terms of deployability, less interesting.

The topology of the mast must have certain static and kinematic properties, which are found using the extended Maxwell's rule:[17]

$$dj - b - c = m - s \tag{1}$$

where d is the dimension of the space, i.e. $d = 2, 3$, j the number of joints, b the number of bars, c the number of kinematic constraints, $c_{\min} = 3(d-1)$, m the number of internal mechanisms and s the number of states of self-stress.

Consider a three-dimensional n-stage tensegrity mast with v struts per stage ($v \geq 3$). The numbers of joints and bars for such a mast are

$$j = 2vn \tag{2}$$

$$b = 2v(3n - 1) \tag{3}$$

Setting $c = c_{\min} = 6$, (1) yields

$$m - s = 2v - 6 \tag{4}$$

which is independent of the number of stages n.[6] Assuming that only one state of self-stress can exist, $s = 1$, the number of mechanisms is

$$m = 2v - 5 \tag{5}$$

The stiffest mast would have three struts per stage, hence $m = 1$. Note that the numbers of states of self-stress s and internal mechanisms m are not constant for a given topology, but depend on the geometry of the structure.

The second step in the design of the mast is the form-finding step, in which a prestressable geometry is sought. Although the topology of this particular mast has been

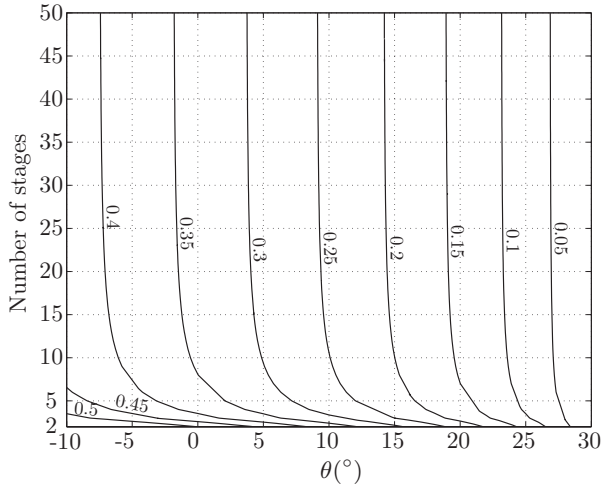

Figure 3: Contour lines of the dimensionless overlap η for multi-stage tensegrity masts with three struts per stage.

known for a long time, the first mathematical form-finding was performed by Sultan.[7] Following Sultan, Nishimura[6] derives a general equation for the overlap $\eta = h/H$ of a two-stage tensegrity mast with v struts per stage. For a two-stage cylindrical mast with three struts per stage the overlap η is given by the following quadratic equation

$$\eta^2 \left(\Theta - \frac{1}{2}\right) - \eta \left(\Theta + \frac{1}{2}\right) + \Theta = 0 \qquad (6)$$

where $\Theta = \cos(\pi/3 + \theta)$.

For multistage masts with constant rotational angle θ throughout, Sultan[7] uses a symbolic approach for the form-finding of masts with maximum nine stages. As the number of stages increases, the computations become too complex for the algebraic manipulation software even though symmetry conditions are used to simplify the equations. Pak[18] develops a numerical approach based on the *Singular Value Decomposition* (SVD) of the equilibrium matrix[19] and analyses masts with up to 15 stages. Tibert[12] modifies the approach by Pak and analyses masts with up to 50 stages. The results are shown in Figure 3. For a given value of θ, the overlap decreases with the number of stages. This is not ideal from a manufacturing point of view as new stages cannot be added without changing the geometry of the whole mast.

Nishimura[6] investigates a class of tensegrity masts with the same self-stress for all stages except the first and the last stages, independent of the total number of stages n. This requires that the end stages have a rotation angle different from that of the interior stages. Thus, the geometry of such a mast is described by three parameters: the rotation angle of the end stages θ, the rotation angle of the interior stages θ^* and the overlap ratio η.

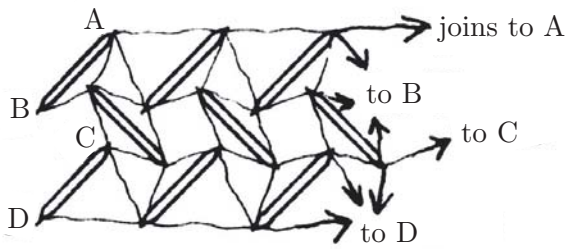

Figure 4: Illustration of Pugh's diamond pattern systems for a three-stage, three struts per stage mast (from Ref. 15).

The relationship between η and θ^* is[6]

$$\eta^2 \left(\frac{1}{2} - \Theta^*\right) + \eta \left(\frac{1}{2} + \frac{\Theta^*}{2}\right) + \frac{\Theta^*}{2} = 0 \qquad (7)$$

where $\Theta^* = \cos(\pi/3 + \theta^*)$. Once θ^* has been specified, η is found by (7). Nishimura[6] subsequently determines the rotation angle of the end stages, θ, by solving a characteristic equation of special matrix. Micheletti[20] later showed that the rotation of the end stages is determined by the condition for the two-stage mast, (6). Hence, (6) and (7) are the only equations needed to find the prestressable configuration of an n-stage tensegrity mast of this particular topology. Note that it is possible to design a mast with the same overlap η and rotation angle $\theta = \theta^*$ but this mast would not be cylindrical; the end radius would be different from the interior radius.

The masts by Nishimura are better suited for practical applications as (i) new stages can be added without changing the geometry of the mast and (ii) the internal forces are relatively uniform throughout.

Manufacturing

As with any other cable structure, a tensegrity mast requires an efficient and accurate manufacturing technique. The conventional way of constructing a mast, i.e. node by node and stage by stage, is inadequate when dealing with flexible members.

The present manufacturing technique, in which the construction of the cables and the struts is separated, is inspired by Pugh's[15] illustration of the diamond pattern system, Figure 4. First, the three-dimensional network of cables is mapped onto a plane without changing any cable lengths. As the cable net is composed mainly of triangles connected according to a particular pattern, the number of net configurations is restricted. In fact, only two configurations, which preserve all cable lengths, exist, see Figure 5(a) and (b).

The two key aspects of the manufacturing method required to obtain good precision are: (i) to ensure accu-

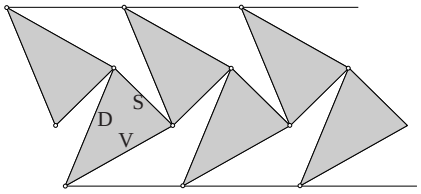

(a) Net 1

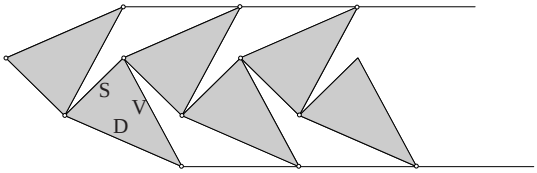

(b) Net 2

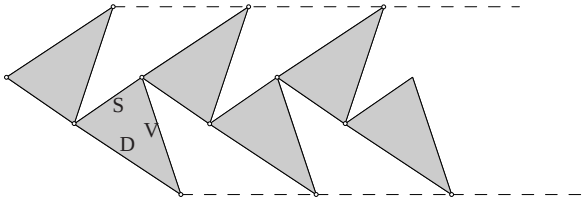

(c) Net 3

Figure 5: Different two-dimensional configurations of two-stage tensegrity masts.

rate element lengths and (ii) to make certain that the angles between cables in the two-dimensional net do not differ too much from the corresponding angles in three dimensions. Net 1 may satisfy the first requirement but certainly not the latter, since the saddle cable is inverted. In this respect net 2 is better, but still not ideal. The horizontal distance between the nodes along the saddles is identical to the length of the base cables, which produces an overlap in two dimensions that is larger than that in three dimensions. By relaxing the length preservation condition slightly, the saddle overlap in the two-dimensional cable net was set equal to ηH, Figure 5(c). In this case the distance between the nodes at the bases is too long and, thus, could not be constructed along with the rest of the net. However, the angles between the members in net 3 agree better with those in three dimensions.

In the two-dimensional net, the cables connected to a node lie in the same plane and go through the same point, Figure 6(a). However, in the three-dimensional net they do not necessarily intersect, Figure 6(b). Thus, the geometry of the mast will change to a configuration where they intersect, i.e. where the forces can be in equilibrium. To eliminate this error source it is necessary to manufacture joints, preferably spherical, with holes drilled in the directions of the cables in the three-dimensional net configuration. By adjusting the distance between the nodes in the two-dimensional net according to the layout of the holes in a spherical joint it would still be possible to construct the net in two dimensions, but the cables will no longer lie in the same plane.

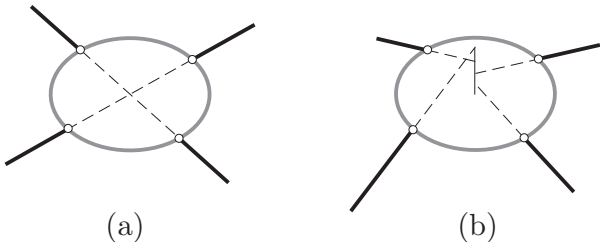

Figure 6: Cables which coincide in two dimensions (a) may not coincide in three dimensions (b).

Deployment

An n-stage tensegrity mast with $3n$ struts has $5 - 2/n$ times more cables than struts. Also, the struts are the longest members and the only stiff ones. Greatest packaging efficiency is therefore achieved with folding struts. Earlier studies of foldable or deployable tensegrity structures have adopted a cable- rather than strut-based folding. Bouderbala and Motro[14] analysed different approaches and found that cable mode folding was less complex than strut mode, although the latter produced a more compact package. Sultan[7] uses an approach in which the cable lengths of all but the base cables are changed so that the structure at every step throughout the deployment is in a stable equilibrium configuration.

Each mode of deployment has its pros and cons. Advantages of the cable mode deployment are:

+ Structure can be stiff during deployment.

+ Slack cables are stored inside the struts to avoid entanglement.

while the disadvantages are:

– Diameter increases during deployment.

– Large number of mechanical devices is needed to control the lengths of the cables.

The advantages and disadvantages of the strut mode of deployment are:

+ Constant diameter throughout deployment,

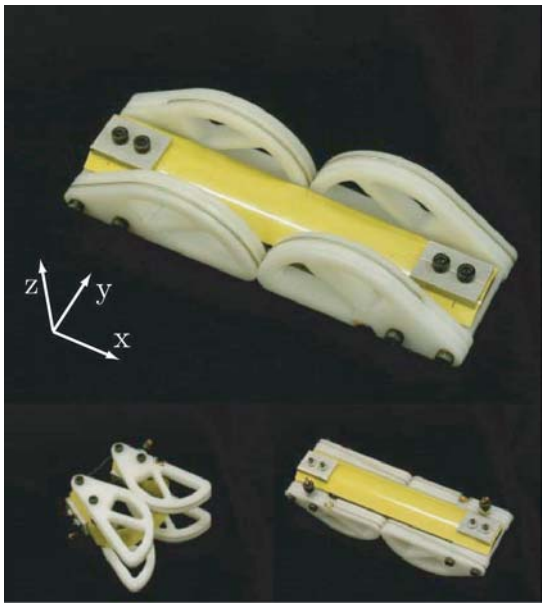

Figure 7: TSR hinge (Courtesy of A.M. Watt)

+ Fewer motors and mechanical devices are needed for deployment

and

– No stiffness until the whole structure has been prestressed—additional stiffening structures are needed.

Here, a strut mode folding is chosen. For a compact package, the struts of each stage must be stacked on top of one another. Such a packaging scheme is possible if the length of each strut is approximately equal to the diameter of the mast and folded using a midpoint hinge. The maximum length of the struts to prevent interference between struts of different stages depends also on the hinge design. Note that it would be possible to collapse the struts into a shorter length if telescopic struts were used. However, the telescopic strut alternative requires a motor on each of the $3n$ struts of the mast; the failure of only one motor ends the deployment.

For the present mast, a compact, self-locking hinge is desired. A reliable hinge with these characteristics has been developed by Watt and Pellegrino.[21] The *Tape Spring Rolamite* (TSR) hinge consists of one or two pairs of steel carpenter tapes connected to a rolling hinge made from plastic wheels connected by steel cables, Figure 7. The advantages of the TSR hinge are the simple assembly and low friction.

To test the manufacturing and deployment procedures, four demonstrator masts were built at various stages in the development process. The last mast built had eight stages, a diameter of 235 mm and a height of 1275 mm. The 275 mm long struts were made of two 6 mm diameter aluminium tubes connected by one pair of 19 mm wide tape springs. A deficiency of a previous demonstrator mast was that the hinged struts were too weak and therefore the mast could not be adequately prestressed to reduce the gravity effects. The new struts were much stiffer in both bending and torsion, and the necessary prestress could be provided.

In the stowed position, the mast was stored in a canister to prevent the struts from snapping back into their straight configuration. An aluminium rod running in the centre of the demonstrator mast was used to activate and control the deployment. For a real application the aluminium rod could be substituted by a *Storable Tubular Extendible Member* (STEM) or an inflatable tube. The complete, sequential deployment of the eight stage mast is shown in Figure 8. The mast is not fully prestressed until the bottom stage is deployed. However, the slender aluminium rod could not provide enough force and the tape spring hinges could not produce enough moment to prestress the whole mast. The final prestressing may be obtained by allowing one of the base cables to be a little longer than required during deployment. All hinges can then deploy without resistance as they do not have to prestress the mast. Finally, the longer base cable is shortened by a motorised turn-buckle which prestresses the mast. Thus, only two motors are needed: one that drives the centre rod and one that shortens the base cable. Although no precaution had been taken to avoid entanglement problems, the deployment of the eight-stage mast had to be stopped only twice.

Structural Analysis

To evaluate the potential of the tensegrity mast as a lightweight, deployable structure a comparison with an existing mast should be done. Currently, one of the most advanced masts for large applications is the *Able Deployable Articulated Mast* (ADAM) by AEC-Able Engineering Company. A 87-stage, 60.68 m long ADAM was used for the *Shuttle Radar Topography Mission* (STRM). This mast had a diameter of 1.12 m, a mass of 290 kg, a bending stiffness of 13 MNm^2 and a fundamental frequency of 0.10 Hz. Naturally, the ADAM would be stiffer than the tensegrity mast as the latter is kinematically indeterminate and lacks continuous longerons. Nevertheless, a stiffness analysis of a tensegrity mast of similar dimensions as the STRM ADAM was done to determine the difference in stiffness.

The mast configuration by Nishimura[6] was chosen as the internal forces were more uniform than for the configuration with equal-length struts throughout. Here, it was assumed that the mast is cylindrical with a constant

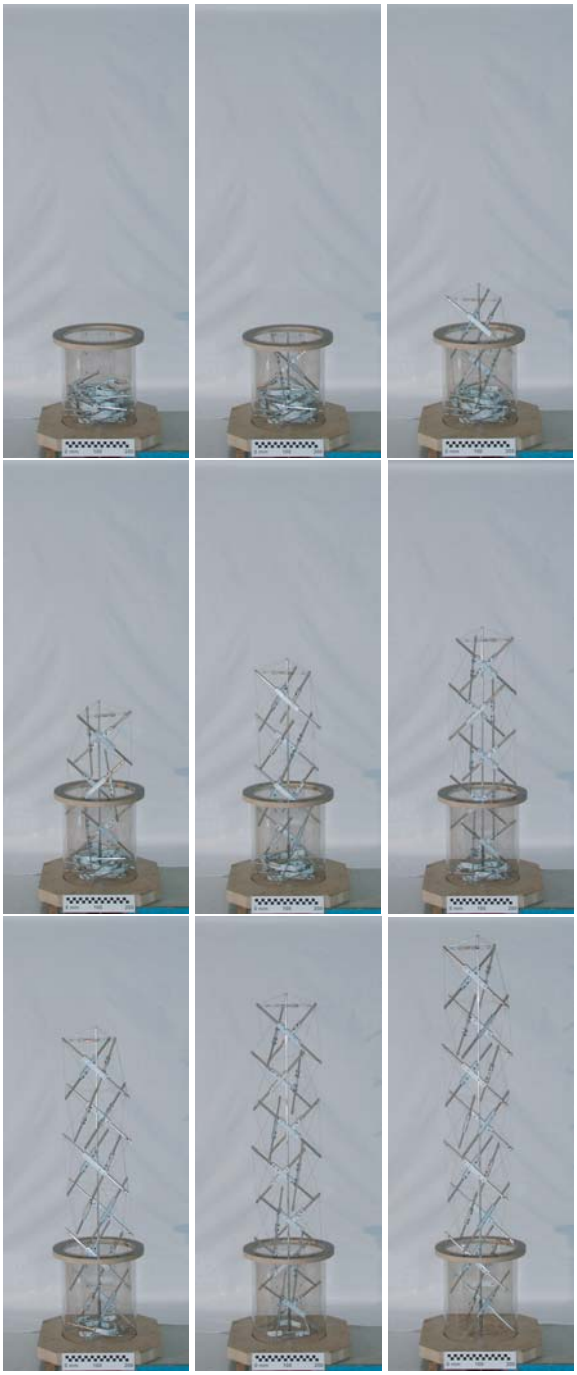

Figure 8: Rod-controlled deployment of eight-stage mast.

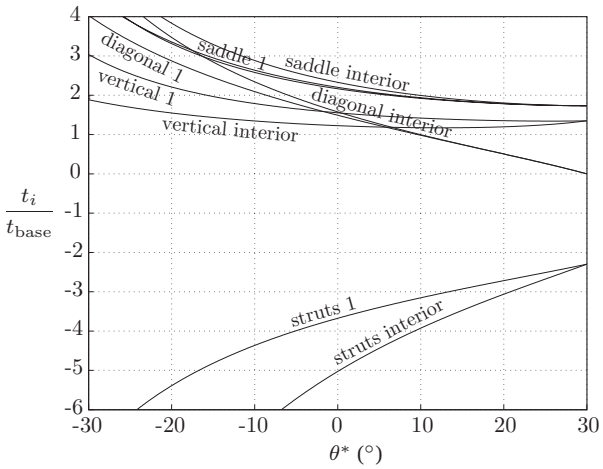

Figure 9: Cable and strut forces in the first (and last) and interior stages in a multi-stage mast with uniform interior forces. $D = 1.12$ m, $H_{\text{bay}} = 0.6975$ m and $n = 87$.

overlap η and two different rotation angles: θ^* for the interior stages and θ for the end stages. Hence, the number of independent force values is nine: strut, vertical, diagonal and two saddle values for the end stages and strut, vertical, diagonal and saddle for interior stages. All values were normalised with respect to the force in the base cables. The variation of these forces with the rotation of the interior stages is shown in Figure 9. The final configuration was based on two criteria: (i) no cable force allowed to be lower than that in the base cables and (ii) the maximum strut force no larger than 5 times the base cable force. This restricts the interval of allowable configurations to 0–10°.

The struts, subjected to the largest forces, were designed as two rigid bars connected by a rotational hinge at midpoint, Figure 10. The buckling load for such a strut is

$$P_{\text{cr}} = 4\frac{C_M}{l} \tag{8}$$

where C_M is the spring stiffness and l the strut length. If the strut is not perfectly straight but has an initial imperfection ψ_{ini}, with the corresponding lateral mid-point displacement $\Delta \approx \psi_{\text{ini}} l/2$, the buckling load becomes

$$P_{\max} = \frac{1}{\dfrac{\Delta}{M_{l/2}} + \dfrac{1}{P_{\text{cr}}}} \tag{9}$$

The buckling moment M_{cr} and stiffness C_M of the TSR hinge are 13 Nm and 480 kNmm/rad, respectively.[21]

At $\theta^* = 0°$, the strut length of the end stages is 1.46 m, which yields $P_{\text{cr}} = 1315$ N using (8). Substituting this load, $\Delta = 3.65$ mm and $M_{l/2} = M_{\text{cr}} = 13$ Nm into (9) yields $P_{\max} = 960$ N. The tubes connected by the hinge were assumed to be made of CFRP with a Young's modulus $E = 210$ GPa and a density $\rho = 1660$ kg/m^3. Minimum wall thickness was set to 1 mm to ensure adequate toughness for handling and assembly. Concerning length precision requirement, the struts cannot be too slender; a strut diameter of 25 mm was assumed. The effective axial stiffness of the hinged strut, taking into account the stiffness of the TSR hinge, was 4.44 kN/mm or 6.49 MN for the 1.46 m strut.

The cables were assumed to be made of thin CFRP

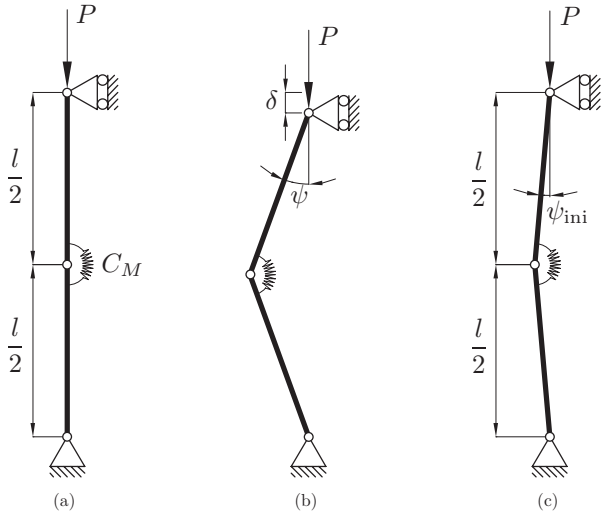

Figure 10: Buckling of a two-link column: (a) initial state, (b) buckled state and (c) initial, imperfect state.

tape 5 mm wide and 0.5 mm thick with the same properties as the tubes. The allowable stress was set to 200 MPa, which provides a safety factor between 5 and 10. Thus, the allowable cable force and axial stiffness were 500 N and 0.53 MN, respectively.

First, a vibration analysis of the mast was performed. In this analysis it was assumed that the mass of each TSR hinge, 0.2 kg, was evenly distributed along the length of each strut. The strut-to-cable joints were assumed to be 25 mm diameter aluminium spheres, each weighing 0.025 kg. The total mass of these joints was distributed along the total length of the struts and the cables. To gain some understanding about the vibrational characteristics of the tensegrity masts, a ten-stage mast with the same diameter and stage height as the 87-stage mast was first analysed. The studied mast had $\theta^* = 10^\circ$. The results for the ten-stage mast is shown in Table 1.

The frequency of the mode corresponding to the "axial" internal mechanism, Figure 11(a), varied with the level of prestress while the bending modes were unaffected. These results agree with those of Murakami.[22] For low prestress levels, the axial mode is the fundamental mode but for longer or more highly prestressed masts, the bending modes have the lowest frequencies. For the 87-stage mast the frequency of the flexural modes is 0.037 Hz, to be compared with 0.10 Hz for the STRM ADAM. The bending stiffness of the tensegrity mast can be computed from the equation for the lowest bending frequency of a cantilever beam:

$$f_{1,\mathrm{cb}} \approx \frac{3.516}{2\pi}\sqrt{\frac{EI}{ml^4}} \qquad (10)$$

The 87-stage tensegrity mast weighs 114.2 kg giving $m = 114.2/60.68 = 1.88$ kg/m. Solving (10) yields

Table 1: Natural frequencies (Hz) of the ten-stage mast. Axial mode frequencies are underlined.

t_{base}	f_1	f_2	f_3	f_4	f_5
50	<u>1.1787</u>	2.8214	2.8468	4.1371	12.0952
100	<u>1.6442</u>	2.8224	2.8478	5.2359	12.6260
200	<u>2.3006</u>	2.8245	2.8499	6.8581	13.5714
500	2.8307	2.8562	<u>3.6006</u>	9.9618	15.6138

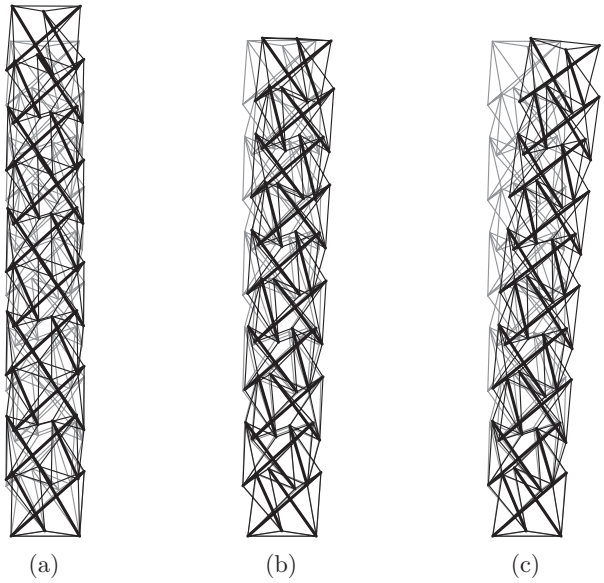

Figure 11: First three eigenmodes of a ten-stage tensegrity mast: (a) $f_1 = 1.179$ Hz, (b) $f_2 = 2.821$ Hz and (c) $f_3 = 2.847$ Hz.

$EI = 0.11$ MNm^2, which should be compared with 13 MNm^2 for the STRM ADAM.

The vibrational analysis above gives information only about the linear behaviour of the mast. To investigate the non-linear behaviour, a static analysis was performed. Earlier studies of slender tensegrity structures, e.g. Ref. 18, indicate that bending strength and stiffness are the critical factors of the tensegrity mast. As for the vibration analysis, the static analysis was done on a ten-stage mast with $\theta^* = 10^\circ$. The mast was modelled by a geometrically non-linear finite element program written in Matlab. The struts were modelled as two-node bar elements and the cables by special no-compression catenary elements. Four load cases were considered: (i) axial tension, (ii) axial compression, (iii) bending in direction 1 and (iv) bending in direction 2, see Figure 12.

As the single internal mechanism makes the mast weak in the axial direction, a way of stiffening the mast was investigated: three additional cables were added to the first stage so that it became fully triangulated. To prestress all the cables of the first stage, a further rotation, i.e. lengthening of the struts, is required. The stiffened

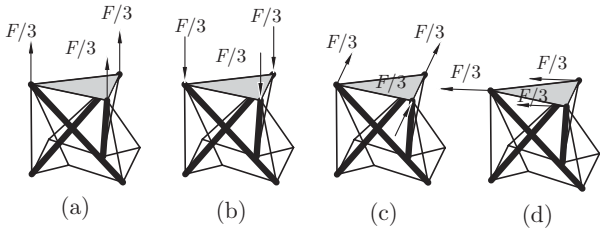

Figure 12: Load cases for the tensegrity mast: (a) tension, (b) compression, (c) bending in direction B1 and (d) bending in direction B2.

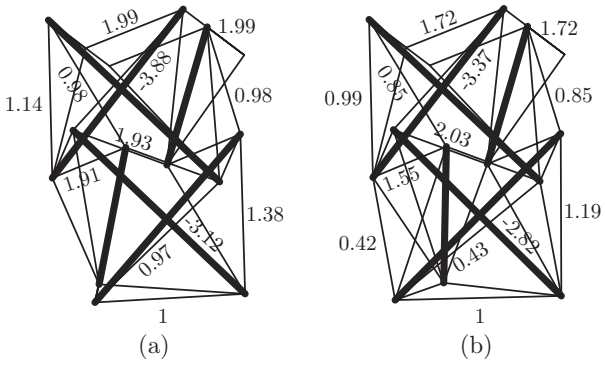

Figure 13: Normalised forces in the two lowest stages of ten-stage tensegrity masts: (a) unstiffened and (b) stiffened.

mast has three independent states of self-stress, $s = 3$, and no internal mechanism. Among the states of self-stress a combination with the same type of symmetry as the mast, i.e. three-fold, may be found. The additional rotation of the bottom stage changes the internal forces of the mast, but not by very much. Figure 13 shows the forces in a normal and a stiffened ten-stage mast with an additional $15°$ rotation of the bottom stage.

Under axial load, the initial behaviour of the unstiffened mast was the same in tension and compression, with a stiffness of 275 kN/m. As the load level increased, the compression stiffness became higher than the tension stiffness, Figure 14. However, the stiffened mast was generally stiffer in tension than in compression although the initial stiffness was about the same, 420 kN/m. At a tensile loading of 16.3 N, three diagonal cables at stage 2 went slack and the stiffness decreased. Under compression load no cable went slack.

For bending loads, the behaviour was different than for axial loads. The initial bending stiffness of the unstiffened mast was 110 kNm^2, as determined by the vibration analysis, for both direction B1 and B2, Figure 15. As the load increased, the diagonal cables on the compression side at stage 2 went slack at 11 N. When this occurred, the stiffness immediately dropped by 80% to 22 kNm^2. The stiffened mast showed a more complex

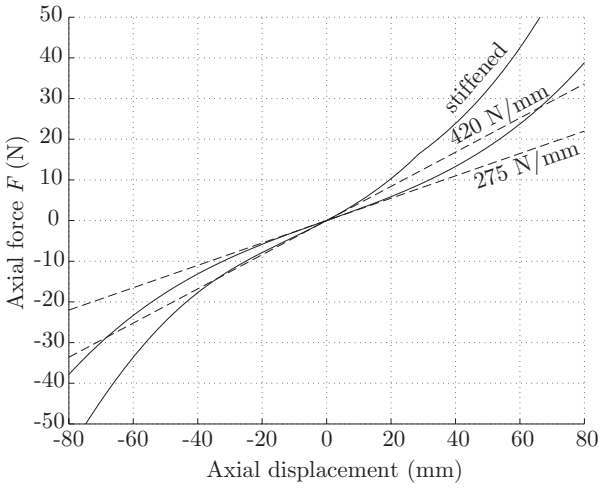

Figure 14: Load–displacement curves for an unstiffened and a stiffened ten-stage tensegrity mast subjected to axial loading.

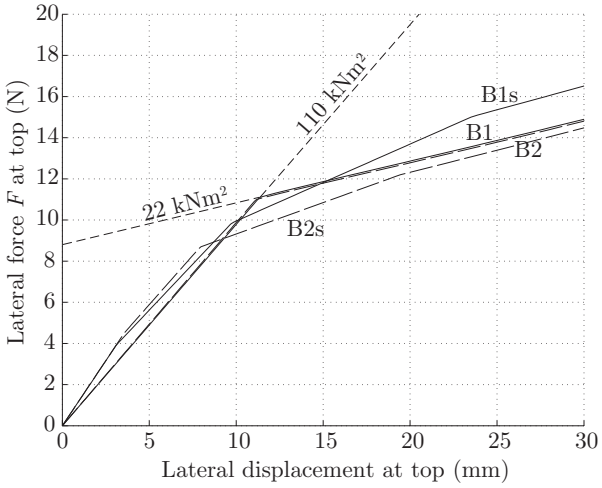

Figure 15: Load–displacement curves for an unstiffened and a stiffened ten-stage tensegrity mast subjected to lateral loading.

behaviour. Initially the stiffness was slightly higher than that of the unstiffened mast, but only up to 4 N when the first cables went slack. Further increase of the load created more and more slack cables and eventually the bending stiffness became equal to that of the unstiffened mast. Also, the behaviour depended on the bending direction. Concerning the low bending strength of the ten-stage mast, it was not necessary to perform a complete analysis of the 87-stage mast.

Discussion

For the chosen topology of the tensegrity mast, the form-finding step was straightforward as closed-form solutions were available.

The manufacturing scheme turned out to be satis-

factory after correcting some early mistakes. Using spherical joints with holes drilled in the correct three-dimensional angles should eliminate the last obvious source of inaccuracy.

Despite the low level of technology of the demonstrator model, the proposed deployment procedure worked well. The major problem is that the mast has no stiffness during deployment. It might be possible to provide full stiffness to the deployed part through a special canister, which would have the role of the struts and prestress the cables. To reduce the risk of the cables getting tangled with the struts during deployment tape-like instead of cord-like cables can be used. Tapes have a natural folding direction and it should be possible to arrange the tapes to avoid interference with the struts.

The structural analysis shows that the masts are relatively stiff axially but weak in bending. The removal of the internal mechanism did not improve the behaviour significantly. The weak bending stiffness is due to the fact that the tensegrity masts do not have continuous longerons, which in conventional masts provide the bending stiffness. The natural way to increase the structural stiffness would be to accept connected struts, but then some other characteristics, e.g. compact packaging, may be lost.

References

[1] K. Miura and S. Pellegrino. *Structural concepts*. Cambridge University Press, Cambridge, UK, (To appear).

[2] R. B. Fuller. Tensile-integrity structures. United States Patent 3,063,521, 1962. Filed 31 August 1959, Granted 13 November 1962.

[3] B. Knight, J. Duffy, C. Crane, and J. Rooney. Innovative deployable antenna developments using tensegrity design. In *41st AIAA/ASME/ASCE/AHS/ASC Structures, Structural Dynamics, and Materials Conference and Exhibit*, pages 984–994, Atlanta, GA, USA, 3–6 April 2000. AIAA 2000-1481.

[4] A. G. Tibert and S. Pellegrino. Furlable reflector concept for small satellites. In *42nd AIAA/ASME/ASCE/AHS/ASC Structures, Structural Dynamics, and Materials Conference and Exhibit*, Seattle, WA, USA, 16–19 April 2001. AIAA 2001-1261.

[5] B. F. Knight. *Deployable antenna kinematics using tensegrity structure design*. PhD thesis, University of Florida, Gainesville, FL, USA, 2000.

[6] Y. Nishimura. *Static and dynamic analyses of tensegrity structures*. PhD thesis, University of California at San Diego, La Jolla, CA, USA, 2000.

[7] C. Sultan. *Modeling, design, and control of tensegrity structures with applications*. PhD thesis, Purdue University, West Lafayette, USA, 1999.

[8] I. Stern. Deployable reflector antenna with tensegrity support architecture and associated methods. United States Patent Application Publication. Pub. no.: US 2002/0190918 A1, Pub. date December 19, 2002.

[9] B. F. Knight, J. Duffy, C. D. Crane, III, and J. Rooney. Deployable antenna using screw motion-based control of tensegrity support architecture. United States Patent 6,441,801. Filed March 30, 2000, Granted August 27, 2002.

[10] R. E. Skelton. Deployable tendon-controlled structure. United States Patent 5,642,590, 1997. Filed October 31 1995, Granted July 1 1997.

[11] A. G. Tibert and S. Pellegrino. Review of form-finding methods for tensegrity structures, 2001. Accepted by *International Journal of Space Structures*.

[12] G. Tibert. *Deployable tensegrity structures for space applications*. PhD thesis, Royal Institute of Technology, Stockholm, Sweden, 2002.

[13] H. Furuya. Concept of deployable tensegrity structures in space application. *International Journal of Space Structures*, 7(2):143–151, 1992.

[14] M. Bouderbala and R. Motro. Folding tensegrity systems. In S. Pellegrino and S. D. Guest, editors, *IUTAM-IASS Symposium on Deployable Structures: Theory and Applications*, pages 27–36, Cambridge, UK, 6–9 September 1998. Kluwer Academic Publishers, Dordrecht, The Netherlands, 2000.

[15] A. Pugh. *An introduction to tensegrity*. University of California Press, Berkeley, CA, USA, 1976.

[16] K. D. Snelson. Continuous tension, discontinuous compression structures. United States Patent 3,169,611, 1965. Filed 14 March 1960, Granted 16 February 1965.

[17] C. R. Calladine. Buckminster Fuller's "tensegrity" structures and Clerk Maxwell's rules for the construction of stiff frames. *International Journal of Solids and Structures*, 14(2):161–172, 1978.

[18] H. Y. E. Pak. Deployable tensegrity structures. Fourth-year undergraduate project report, 24 May 2000. Department of Engineering, University of Cambridge, Cambridge, UK.

[19] S. Pellegrino. Structural computations with the singular value decomposition of the equilibrium matrix. *International Journal of Solids and Structures*, 30(21):3025–3035, 1993.

[20] A. Micheletti. On the kinematics of tensegrity towers. Oral presentation at "Colloquium Lagrangianum—Strutture Tensegrity: Analisi e Progetti", 6–8 May 2001, Rome, Italy.

[21] A. M. Watt and S. Pellegrino. Tape-spring rolling hinges. In *Proceedings of the 36th Aerospace Mechanisms Symposium*, Glenn Research Center, Cleveland, OH, USA, 15–17 May 2002. NASA.

[22] H. Murakami. Static and dynamic analyses of tensegrity structures. Part I. Nonlinear equations of motion. *International Journal of Solids and Structures*, 38:3599–3613, 2001.